

1 **A high-throughput method for measuring critical thermal limits of**  
2 **leaves by chlorophyll imaging fluorescence**

3

4 Pieter A. Arnold<sup>1,\*</sup>, Verónica F. Briceño<sup>1</sup>, Kelli M. Gowland<sup>1</sup>, Alexandra A. Catling<sup>1</sup>,  
5 León A. Bravo<sup>2</sup>, Adrienne B. Nicotra<sup>1</sup>

6

7 <sup>1</sup> Division of Ecology and Evolution, Research School of Biology, The Australian National  
8 University, Canberra, ACT, Australia

9 <sup>2</sup> Department of Agronomical Sciences and Natural Resources, Faculty of Agropecuary and  
10 Forestry Sciences & Center of Plant, Soil Interaction and Natural Resources Biotechnology,  
11 Scientific and Technological Bioresource Nucleus, Universidad de La Frontera, Casilla 54D,  
12 Temuco, Chile

13

14 \*Corresponding author: Pieter A. Arnold, address: 46 Sullivans Creek Rd, Acton, ACT 2600,  
15 Australia, email: [pieter.arnold@anu.edu.au](mailto:pieter.arnold@anu.edu.au), phone: +61 2 6125 2543

16

17 **Running head:** Leaf thermal limits using chlorophyll fluorimetry

18

19 **Keywords:** Chlorophyll fluorescence, cold tolerance, ecophysiology, physiological ecology,  
20 temperature stress

21 **Abstract**

22 Plant thermal tolerance is a crucial research area as the climate warms and extreme weather  
23 events become more frequent. Leaves exposed to temperature extremes have inhibited  
24 photosynthesis and will accumulate damage to photosystem II (PSII) if tolerance thresholds are  
25 exceeded. Temperature-dependent changes in basal chlorophyll fluorescence ( $T-F_0$ ) can be used  
26 to identify the critical temperature at which PSII is inhibited. We developed and tested a high-  
27 throughput method for measuring the critical temperatures for PSII at low ( $CT_{MIN}$ ) and high  
28 ( $CT_{MAX}$ ) temperatures using a Maxi-Imaging fluorimeter and a thermoelectric Peltier plate  
29 heating/cooling system. We examined how experimental conditions: wet *vs* dry surfaces for  
30 leaves and heating/cooling rate, affect  $CT_{MIN}$  and  $CT_{MAX}$  across four species.  $CT_{MAX}$  estimates  
31 were not different whether measured on wet or dry surfaces, but leaves were apparently less  
32 cold tolerant when on wet surfaces. Heating/cooling rate had a strong effect on both  $CT_{MAX}$  and  
33  $CT_{MIN}$  that was species-specific. We discuss potential mechanisms for these results and  
34 recommend settings for researchers to use when measuring  $T-F_0$ . The approach that we  
35 demonstrated here allows the high-throughput measurement of a valuable ecophysiological  
36 parameter that estimates the critical temperature thresholds of leaf photosynthetic performance  
37 in response to thermal extremes.

## 38 **Introduction**

39 Understanding both vulnerability and tolerance limits of plants to thermal extremes is a priority  
40 for plant biology research as the Earth's climate continues to change, thereby exposing these  
41 sessile organisms to increased thermal stress (O'Sullivan *et al.* 2017; IPCC 2018; Geange *et al.*  
42 2021). Thermal stress disrupts and inhibits physiological processes (Goraya *et al.* 2017), induces  
43 protective and repair mechanisms (Sung *et al.* 2003; Goh *et al.* 2012), leads to declines in plant  
44 performance, and threatens survival (Zinn *et al.* 2010; Bita and Gerats 2013). Plant  
45 photosynthesis is sensitive to thermal stress and has distinct limits beyond which photosynthetic  
46 assimilation is inhibited and tissue damage can occur (e.g., Neuner and Pramsohler 2006;  
47 Sukhov *et al.* 2017). The temperature sensitivity of photosynthesis is in part derived from the  
48 thermally-dependent stability of protein-pigment complexes in the light harvesting complex II  
49 (LHCII) of photosystem II (PSII) of the thylakoid membrane in chloroplasts (Ilík *et al.* 2003),  
50 which are integral to the photosynthetic electron transport chain (Berry and Björkman 1980;  
51 Allakhverdiev *et al.* 2008; Mathur *et al.* 2014).

52 Chlorophyll fluorimetry has become a widely used tool for assessing the thermal limits  
53 of photosynthesis for both cold and heat tolerance (Geange *et al.* 2021). Chlorophyll can  
54 dissipate absorbed light energy via photochemistry or re-emit it as heat energy or fluorescence  
55 (Baker 2008; Murchie and Lawson 2013). A dark-adapted leaf exposed to a low-intensity  
56 modulated measuring light, which does not induce electron transport, emits a minimal amount  
57 of chlorophyll-*a* fluorescence from LHCII, called  $F_0$  (Yamane *et al.* 1997). Under more intense  
58 or actinic light, processes that are highly dynamic and sensitive to other factors but not well  
59 correlated with the viability of the photosynthetic tissue cannot be isolated from the  
60 measurement of the temperature dependence (thermal stability) of chlorophyll fluorescence  
61 (Schreiber *et al.* 1995; Logan *et al.* 2007). To assess the thermal stability limits of LHCII, plant  
62 ecophysicists typically measure the temperature-dependent change in basal chlorophyll-*a*  
63 fluorescence ( $T-F_0$ ) to determine the critical temperature threshold ( $T_{\text{crit}}$ ), denoted by a sudden  
64 increased in  $F_0$  at which PSII begins to inactivate (e.g., Schreiber and Berry 1977; Berry and  
65 Björkman 1980; Briantais *et al.* 1996; Knight and Ackerly 2002; Ilík *et al.* 2003; Hüve *et al.*  
66 2006; Neuner and Pramsohler 2006; O'Sullivan *et al.* 2013; O'Sullivan *et al.* 2017; Zhu *et al.*  
67 2018).  $F_0$  is a fluorescence parameter that can be measured rapidly and continuously throughout  
68 heating or cooling in darkness, without the need of a saturating pulse and re-dark adaptation as  
69 for  $F_v/F_M$  measurements that are commonly used to detect photosynthetic inhibition.

70 One critique of  $T-F_0$  measurements and  $T_{\text{crit}}$  determination is that they are conducted on  
71 detached leaves. Detaching leaves to expose them to a precisely controlled and measured

72 thermal surface is usually, but not always, a necessary component of this trait measurement.  
73 While modern chlorophyll fluorescence imaging systems can be used on attached leaves,  
74 simultaneously heating or cooling these leaves precisely while measuring multiple leaf samples  
75 remains logically complex, especially for ecological applications. Leaf detachment can affect  
76 leaf hydration and fluorescence through reduced PSII activity, ionic leakage, and oxidations  
77 compared to attached leaves (Potvin 1985; Smillie *et al.* 1987). Leaf dehydration could be  
78 problematic for certain species if leaves are sampled long before they are assessed for  $T_{\text{crit}}$  or if  
79 they are measured as leaf sections or discs. To avoid dehydration during the  $T\text{-}F_0$  measurement,  
80 a wet surface, such as damp paper surface as in Knight and Ackerly (2002), could physically  
81 impair evaporation by saturating the atmosphere surrounding the leaf. However, it is not clear  
82 whether a wet surface interferes with the  $T\text{-}F_0$  measurement or how it might affect the  $T_{\text{crit}}$  value  
83 compared to using a dry surface.

84 A great advantage of using temperature-dependent changes in chlorophyll fluorescence  
85 and a thermoelectric plate is that both cold and heat tolerance limits of leaves can be measured  
86 with much of the same equipment. However, the protocol may need to be altered slightly  
87 because cold transitions in nature occur much more slowly than heat transitions, which may  
88 induce different mechanisms in response to thermal stress. For example, leaf temperature can  
89 rapidly increase during a lull in wind speed, far exceeding ambient temperature on a hot and  
90 sunny day (Vogel 2009; Leigh *et al.* 2012). On a cold frosty night, even considering air  
91 temperature stratification, the rate of leaf temperature cooling rarely exceeds  $5^{\circ}\text{C h}^{-1}$ , especially  
92 below freezing (Sakai and Larcher 1987). Therefore, the ‘standard’ protocols for measuring  $T_{\text{crit}}$   
93 typically change temperature much faster for heat tolerance than for cold tolerance. While this  
94 approach is justified by rates observed in natural systems, the first published application of the  
95  $T\text{-}F_0$  technique (Schreiber and Berry 1977) used an apparently arbitrary ‘slow’ heating rate of  
96  $1^{\circ}\text{C min}^{-1}$  (i.e.,  $60^{\circ}\text{C h}^{-1}$ ). Subsequently, while many studies followed suit, a vast range of  
97 heating/cooling rates have been applied (see Table S1, available as Supplementary Material to  
98 this paper), often with little justification. We have known for decades that different rates of  
99 heating and cooling can affect the  $T\text{-}F_0$  curve and shift the  $T_{\text{crit}}$  value by at least  $2^{\circ}\text{C}$  (Bilger *et*  
100 *al.* 1984; Frolec *et al.* 2008). Therefore, studies employing  $T\text{-}F_0$  methods for measuring thermal  
101 tolerance limits that use different heating/cooling rates might not be directly comparable, even  
102 within a given species. Further, it is reasonable to expect that plant species might exhibit  
103 different responses to variation in methodology.

104 Here, we present a practical, high-throughput method for measuring  $T_{\text{crit}}$  with a Pulse  
105 Amplitude Modulated (PAM) chlorophyll fluorescence imaging system that measures  $F_0$  in real

106 time as a thermoelectric Peltier plate with leaf samples is heated or cooled to thermal extremes.  
107 We then investigate variations of easily controllable variables of the standard experimental  
108 protocol that could affect thermal tolerance limit estimates. We sought to determine the effects  
109 of wet vs dry surface and heating/cooling rate on  $T_{\text{crit}}$  estimates for both the heat tolerance limit  
110 (hereafter referred to as critical maximum temperature;  $CT_{\text{MAX}}$ ) and the cold tolerance limit  
111 (hereafter referred to as critical minimum temperature;  $CT_{\text{MIN}}$ ) of leaf thermal stability of  
112 species with different growth forms. By comparing among these species, we also determined  
113 whether the effects of the two experimental variables could be generalised for different growth  
114 forms of plants that originate from different conditions. In doing so, we advise researchers on  
115 what we consider to be a pragmatic approach to measuring leaf thermal tolerance using  
116 chlorophyll imaging fluorescence, at a time when improved understanding of plant tolerance to  
117 thermal extremes is needed for cultivated and wild species alike.

118

## 119 **Materials and Methods**

### 120 *Species description and leaf samples*

121 We chose plant species that represented diverse growth habits and leaf morphology (in surface  
122 characteristics and leaf thickness) to make simple interspecific comparisons while testing the  $T$ -  
123  $F_0$  method. *Wahlenbergia ceracea* Lothian (Campanulaceae) waxy bluebell is a small perennial  
124 herb that is sparsely distributed across south-eastern Australia. We grew F2 generation  
125 *W. ceracea* plants under controlled glasshouse conditions (20/15°C set day/night temperatures)  
126 and leaves from mature plants were used for all experiments. Seed stock originated from  
127 Kosciuszko National Park, NSW, Australia (36.432°S, 148.338°E) that was collected in 2015  
128 and 2016. *Melaleuca citrina* (Curtis) Dum. Cours. (Myrtaceae) common red bottlebrush were  
129 used for all experiments. This species is native to south-eastern Australia but also distributed as  
130 a cosmopolitan plant. Sampled individuals were growing as native shrubs at The Australian  
131 National University, ACT, Australia (35.279°S, 149.118°E). *Quercus phellos* L. (Fagaceae)  
132 willow oak trees were used only in the heat tolerance component of the surface wetness  
133 experiment, prior to the abscission of leaves in autumn. This deciduous species is native to  
134 North America and sampled individuals were growing as tall, shady ornamental trees at The  
135 Australian National University, ACT, Australia (35.277°S, 149.115°E). *Escallonia rubra* var.  
136 'pink pixie' (Ruiz & Pav.) Pers. (Escalloniaceae) pink escallonia were used for the cold  
137 tolerance component of the surface wetness experiment and the heating/cooling rate experiment  
138 in place of *Q. phellos* after the former shed its leaves. *Escallonia rubra* is native to South

139 America and sampled individuals were growing as dense ornamental shrubs at The Australian  
140 National University, ACT, Australia (35.277°S, 149.117°E).

141 All measurements were taken between February and October 2019. Due to the variation  
142 in species availability across experiments and the potential effects of seasonal change on  
143 absolute tolerance values, we consider each experiment separately and do not draw comparisons  
144 across surface wetness and heating/cooling rate experiments. Assays (surface wetness or  
145 heating/cooling rates for heat or cold tolerance assays) were conducted on replicate days to  
146 control for potential effects of day. Leaves selected for measurement were fully expanded,  
147 visually free of damage and discolouration, and within two leaf pairs of a growing stem tip on  
148 an intact and healthy stem. Although leaf age could not be determined directly, these criteria  
149 allowed us to select leaves from the same cohort and of similar condition. Leaves were excised  
150 between 0900 and 1300 hours, placed in sealed bags, and then taken to the lab in an insulated  
151 container, where they were always used for  $T-F_0$  measurements within 30 minutes of initial  
152 collection.

153

154 ***Temperature-dependent change in chlorophyll fluorescence ( $T-F_0$ ) measurement***

155 Leaf samples were attached to white filter paper (125 × 100 mm) with double-sided tape. We  
156 placed the filter paper with leaves on a Peltier plate (CP-121HT; TE-Technology, Inc.,  
157 Michigan, USA; 152 × 152 mm surface) that was controlled by a bi-polar proportional-integral-  
158 derivative temperature controller (TC-36-25; TE-Technology, Inc.) and powered by a fixed-  
159 voltage power supply (PS-24-13; TE-Technology, Inc.). The Peltier plate uses four direct-  
160 contact thermoelectric modules that can both cool and heat the plate, which with a MP-3193  
161 thermistor (TE-Technology, Inc.) the plate had potential thermal limits of -20°C and 100°C.  
162 LabVIEW-based control software (National Instruments, Texas, USA) was adapted to control  
163 heating or cooling rate using source code available from TE-Technology, Inc. based on the  
164 supplied user interface. The Peltier plate maintained a stable set temperature within  $\pm 0.1^\circ\text{C}$   
165 (precision) and  $\pm 1^\circ\text{C}$  tolerance across the plate surface. We attached two type-T thermocouples  
166 to the underside of two randomly selected leaves on the plate as representative measures of leaf  
167 temperatures. Thermocouple temperature data were recorded every 10 s by a dual-channel data  
168 logger (EL-GFX-DTC; Lascar Electronics Ltd., Salisbury, UK) and the mean temperature of the  
169 two thermocouples was used for all leaf temperature calculations. Because the two  
170 thermocouples measured temperatures of two single leaves per experimental run, we were able  
171 to extract a small subset of ice nucleation temperatures ( $NT$ ) using the temperature of the first  
172 exothermic reaction in cold tolerance assays. The Peltier plate assembly height was controlled

173 by a laboratory scissor-jack to fit within an aluminium frame at an ideal height below the  
174 fluorescence camera (Fig. 1a). Heavy double-glazed glass was placed on top of the leaf samples  
175 on the plate to compress samples against the plate surface to ensure maximum contact and  
176 create a thermal buffer to ensure close matching of leaf and plate temperatures. In addition to  
177 greater thermal buffering relative to standard glass, double-glazed glass avoids condensation  
178 that might lead to erroneous measurements of  $F_0$ . All areas of both the Peltier plate and glass  
179 that were outside of the filter paper area were blacked out with heat-resistant black electrical  
180 tape to remove ambient light reflection and interference.

181 We used a Pulse Amplitude Modulated (PAM) chlorophyll fluorescence imaging system  
182 (Maxi-Imaging-PAM; Heinz Walz GmbH, Effeltrich, Germany) mounted 185 mm above the  
183 Peltier plate (imaging area of approximately 120 × 90 mm) to measure fluorescence parameters.  
184 A weak blue pulse modulated measuring light (0.5  $\mu\text{mol photons m}^{-2} \text{ s}^{-1}$ ) was applied  
185 continuously at low frequency (1 Hz) to measure basal chlorophyll fluorescence ( $F_0$ ) from the  
186 LHCII without driving PSII photochemistry. A red Perspex hood filtered ambient light from the  
187 samples and the camera, and the entire Maxi-Imaging-PAM assembly was covered by thick  
188 black fabric so that all measurements were made in darkness. Leaves were dark adapted for  
189 30 minutes to oxidise all PSII acceptors and obtain the basal  $F_0$  values and then a single  
190 saturating pulse at 10,000  $\mu\text{mol photons m}^{-2} \text{ s}^{-1}$  was applied for 720 ms to determine the  
191 maximal fluorescence ( $F_M$ ) when the photosystem reaction centres are closed. Variable  
192 fluorescence ( $F_V$ ) was calculated as  $F_M - F_0$  and the relative maximum quantum yield of PSII  
193 photochemistry ( $F_V/F_M$ ) was derived.  $F_V/F_M$  is frequently used as a rapid measurement of stress  
194 or relative health of leaves, where optimal  $F_V/F_M$  values of non-stressed leaves are around 0.83  
195 (Baker 2008; Murchie and Lawson 2013). Because our intention was to compare methods, we  
196 aimed for a uniform sample of leaves, and therefore we used  $F_V/F_M$  values  $> 0.65$  to subset data  
197 to exclude any damaged leaves and focus on the  $T-F_0$  of only healthy leaves. This conservative  
198 sample exclusion process resulted in some experimental conditions or species with uneven and  
199 lower sample sizes.

200 In each assay, we selected circular areas of interest that were as large as could fit within  
201 the boundaries of each leaf using the Maxi-Imaging-PAM software, such that the  $F_0$  values were  
202 measured on the widest part of each leaf. One minute after measuring  $F_V/F_M$ , the  
203 heating/cooling program was started simultaneously with the continuous recording of  $F_0$  values  
204 at set intervals with specifics varying depending on duration of the assay reflecting memory  
205 capacity limits of the Maxi-Imaging-PAM (see below). For hot  $T-F_0$  measurements, the initial  
206 set temperature held for dark adaptation of the leaves and  $F_V/F_M$  was 20°C, which was then

207 heated to 60°C at varying rates (see heating/cooling rate experiment). For cold  $T\text{-}F_0$   
208 measurements, the assays were conducted in a cold room (set temperature:  $4 \pm 2^\circ\text{C}$ ) so that the  
209 Peltier plate could reach  $-20^\circ\text{C}$ . At ambient room temperatures of  $\sim 20\text{--}22^\circ\text{C}$ , the Peltier plate  
210 can reach approximately  $-14^\circ\text{C}$  before the plate heat output restrains cooling capacity. The  
211 initial set temperature held for dark adaptation of the leaves and  $F_V/F_M$  was  $4^\circ\text{C}$ , which was then  
212 cooled down to  $-20^\circ\text{C}$ .

213 The  $T\text{-}F_0$  curve produced by heating/cooling the Peltier plate (and leaf samples) is  
214 characterised by a stable or slow-rise in  $F_0$  values until a critical temperature threshold where  
215 there is a fast rise in  $F_0$ . With temperature on the  $x$ -axis and  $F_0$  on the  $y$ -axis, the inflection point  
216 of extrapolated regression lines for each of the slow and fast rise phases of the temperature-  
217 dependent chlorophyll fluorescence response is the critical temperature,  $T_{\text{crit}}$  (Knight and  
218 Ackerly 2002; Neuner and Pramsohler 2006). The term  $T_{\text{crit}}$  is ambiguous outside of this context  
219 when both hot and cold thermal tolerance assays are conducted within the same study.  
220 Hereafter, we refer to  $T_{\text{crit}}$  only as the temperature extrapolated at the inflection point, and  
221 elsewhere use accepted nomenclature used in thermal biology,  $CT_{\text{MAX}}$  and  $CT_{\text{MIN}}$ , as upper  
222 (heat) and lower (cold) thermal limits of leaf thermal tolerance (e.g., Sinclair *et al.* 2016; Janion-  
223 Scheepers *et al.* 2018). Figure 1 presents representative  $T\text{-}F_0$  curves and the calculations of  $T_{\text{crit}}$   
224 values for freezing leaves, where the fast rise phase occurs abruptly (Fig. 1b), and for heating  
225 leaves where the fast rise phase is relatively gradual (Fig. 1c). The inflection point was  
226 calculated using a break-point regression analysis of the mean leaf temperature estimated from  
227 two thermocouples attached to leaves on the plate and relative  $F_0$  values using the *segmented* R  
228 package (Muggeo 2017) using the R Environment for Statistical Computing (R Core Team  
229 2020). We provide example files and example R code for extracting  $T_{\text{crit}}$  values from  $T\text{-}F_0$   
230 curves at <https://github.com/pieterarnold/Tcrit-extraction>.

231  
232 **Surface wetness experiment: effect of wet vs dry surfaces for leaves on  $CT_{\text{MIN}}$  and  $CT_{\text{MAX}}$**   
233 Most experiments that measure  $T\text{-}F_0$  have measured leaf samples with all excess surface  
234 moisture removed, on a dry surface. However, maintaining water content of detached leaves by  
235 providing a wet surface where leaves were placed on top could be a viable way to facilitate  
236 water uptake and keep leaf samples hydrated. In our experiment, leaves were placed on a filter  
237 paper surface. For the wet surface treatment, leaves were placed as described above and then the  
238 filter paper was saturated with MilliQ water-soaked paper towels with excess water absorbed  
239 with dry paper towel thereafter. We compared  $T\text{-}F_0$  curves and  $T_{\text{crit}}$  estimates for both heat and  
240 cold tolerance assays at a heating/cooling rate of  $60^\circ\text{C h}^{-1}$  where leaves were placed on top of

241 either wet or dry filter paper surfaces. A small subset of leaves on wet and dry surfaces were  
242 also measured for  $CT_{MIN}$  and  $NT$  at  $15^{\circ}\text{C h}^{-1}$  in addition to the  $60^{\circ}\text{C h}^{-1}$  experiment.

243

244 ***Heating/cooling rate experiment: effect of heating/cooling rate on  $CT_{MAX}$  and  $CT_{MIN}$***

245 Studies on thermal tolerance limits vary substantially in their set heating/cooling rate (Table S1),  
246 ranging from 30 to  $> 600^{\circ}\text{C h}^{-1}$  in studies on heat tolerance limits ( $CT_{MAX}$ ) and from 1 to  
247  $10^{\circ}\text{C h}^{-1}$  in studies on cold or freezing tolerance limits ( $CT_{MIN}$ ). The difference in magnitude  
248 between heat and cold tolerance limits reflects differences in natural potential rates of heating  
249 and cooling, where leaves may rapidly increase in temperature ( $> 240^{\circ}\text{C h}^{-1}$  for a short period  
250 (Vogel 2009)) but cooling occurs far more slowly (rarely exceeding  $5^{\circ}\text{C h}^{-1}$  (Buchner and  
251 Neuner 2009)). It stands to reason that the more than 10-fold difference in heating or cooling  
252 rates used among studies would affect the estimates and thus comparability of  $T_{crit}$ , but this  
253 effect is not well understood. We chose a wide range of heating/cooling rates for both hot and  
254 cold with the aim to determine how the  $T_{crit}$  estimate for  $CT_{MIN}$  and  $CT_{MAX}$  changes with  
255 heating/cooling rate. We compared  $T-F_0$  curves and  $T_{crit}$  estimates from different heating/cooling  
256 rates for both heat ( $6, 15, 30, 45, 60, 120, 240^{\circ}\text{C h}^{-1}$ ) and cold ( $3, 6, 15, 30, 60, 240^{\circ}\text{C h}^{-1}$ )  
257 tolerance assays where the filter paper was dry, and measurements were conducted in darkness.  
258 For  $240, 60$ , and  $30^{\circ}\text{C h}^{-1}$  heating/cooling rates,  $F_0$  was recorded at 10 s intervals, 20 s for 15  
259 and  $6^{\circ}\text{C h}^{-1}$  heating/cooling rates, and 30 s for  $3^{\circ}\text{C h}^{-1}$  heating/cooling rates due to the 1000  
260 record limit after which the Maxi-Imaging-PAM software stops recording.

261

262 ***Statistical analyses***

263 The dataset was trimmed by removing leaves that had initial  $F_V/F_M$  values below 0.65, which  
264 was a value chosen to identify and remove unhealthy or damaged leaves, hence sample sizes  
265 varied among species and experimental conditions. Summary data (mean  $\pm$  standard error) is  
266 reported in Table S2. Data that matched conditions used in all experiments were used for  
267 multiple analyses (e.g., hot assay, heating/cooling rate of  $60^{\circ}\text{C h}^{-1}$ , dry filter paper could be used  
268 for all). Linear regression models were implemented using the *stats* package in the R  
269 environment for statistical and graphical computing (v3.5.1) (R Core Team 2020). Models were  
270 specified with  $CT_{MIN}$  or  $CT_{MAX}$  as the response variable and fixed categorical predictors of  
271 either wet/dry or heating/cooling rate depending on the experiment.  $F_V/F_M$  was always included  
272 as a fixed covariate. We first fit models combining the three species for a given experiment, and  
273 then we fit species-specific models. Preliminary models were linear mixed effects regression  
274 models that included individual plant as a random factor, but in almost all cases, the term

275 explained essentially zero variance, so we removed the random term in favour of a simpler  
276 linear model. Tables report model parameter estimates with statistical significance at  $p < 0.05$   
277 indicated in bold and with \* symbols. Supplementary tables (Tables S3–S6) report full statistical  
278 model output. Figures show means with non-parametric bootstrapped 95% confidence intervals  
279 (95% CIs) derived from the *Hmisc* R package (Harrell 2019). Finally, predicted temperature  
280 threshold estimates were modelled as a quadratic function of heating/cooling rate treated as a  
281 continuous variable for visualisation purposes. The data that support the findings of this study  
282 are openly available in the figshare repository: [10.6084/m9.figshare.12545093](https://doi.org/10.6084/m9.figshare.12545093).

283

## 284 **Results**

### 285 *Overview*

286 The Peltier plate and chlorophyll fluorescence Maxi-Imaging-PAM system allows us to measure  
287  $T-F_0$  (Fig. 1) on many leaves simultaneously. In these experiments, we measured up to 30 whole  
288 leaf samples in a single experimental run, which could take as little as 90 minutes including dark  
289 adaptation, leaf set up on the surface, and the temperature heating/cooling rate (at  $60^{\circ}\text{C h}^{-1}$ ). The  
290 Peltier plate can easily accommodate a much greater number of smaller leaves, leaf discs, or leaf  
291 sections for even higher throughput phenotyping if required (Fig. S1).

292

### 293 *Surface wetness experiment: effect of wet vs dry surface for leaves on $CT_{\text{MIN}}$ and $CT_{\text{MAX}}$*

294 The effect of water saturating the filter paper was clearly apparent for  $T_{\text{crit}}$  value estimates for  
295  $CT_{\text{MIN}}$  (Fig. 2a) but not  $CT_{\text{MAX}}$  (Fig. 2b). For all species combined and when the three species  
296 were analysed separately,  $CT_{\text{MIN}}$  values were significantly and consistently less negative (less  
297 cold tolerant) for leaves on wet surfaces than on dry ones, by  $3\text{--}4^{\circ}\text{C}$  (Table 1, S3, Fig. 2a).  
298 Variation in  $CT_{\text{MIN}}$  was independent of the initial  $F_{\text{V}}/F_{\text{M}}$  of leaves. The  $CT_{\text{MAX}}$  of leaves with a  
299 wet paper surface did not differ significantly from dry ones both among and within species (all  
300  $p > 0.2$ ; Table 1, S3, Fig. 2b), although the three species had different  $CT_{\text{MAX}}$  estimates. Leaves  
301 with higher  $F_{\text{V}}/F_{\text{M}}$  had higher  $CT_{\text{MAX}}$  for *W. ceracea*.

302

### 303 *Surface wetness $\times$ heating/cooling rate experiment: effects on $CT_{\text{MIN}}$ and $NT$*

304  $CT_{\text{MIN}}$  of leaves of all species was higher on a wet surface and generally lower at faster cooling  
305 rates compared to leaves on a dry surface at slower cooling rate (Table S4). However, the  
306 interaction between surface wetness and cooling rate never had a significant effect on  $CT_{\text{MIN}}$ ;  
307 leaves on a wet surface had a consistently higher  $CT_{\text{MIN}}$  than those on a dry surface at both 15  
308 and  $60^{\circ}\text{C h}^{-1}$ . A small subset of 17 leaves could be used to test whether surface wetness and

309 cooling rates affected  $NT$ , however, due to this low sample size, we opted not to formally  
310 analyse these data, but present descriptive findings in Fig. S2.  $NT$  of leaves measured on a wet  
311 surface occurred at higher temperatures (around  $-7^{\circ}\text{C}$ ) independently of cooling rate, however  
312  $NT$  occurred at lower temperatures on leaves on a dry surface, and perhaps slightly lower on  
313 leaves exposed to a faster cooling rate (Fig. S2).  $NT$  generally occurred at temperatures  $2\text{--}4^{\circ}\text{C}$   
314 higher than  $CT_{\text{MIN}}$ , and the mean difference between  $CT_{\text{MIN}}$  and  $NT$  was  $1^{\circ}\text{C}$  lower on a wet  
315 surface compared to a dry surface (Fig. S2).

316

317 ***Heating/cooling rate experiment: effect of heating/cooling rate on  $CT_{\text{MAX}}$  and  $CT_{\text{MIN}}$***

318 Varying heating/cooling rate affected the estimate of  $T_{\text{crit}}$  for  $CT_{\text{MIN}}$  and  $CT_{\text{MAX}}$  considerably,  
319 however each species responded differently. For  $CT_{\text{MIN}}$ , slow cooling rates ( $< 10^{\circ}\text{C h}^{-1}$ ) are  
320 standard practice and here we used  $3^{\circ}\text{C h}^{-1}$  as the reference category. We found no significant  
321 differences between 3, 6, 15, or  $30^{\circ}\text{C h}^{-1}$  cooling rates overall, but when the plate was cooled at  
322 faster rates, the  $CT_{\text{MIN}}$  values became very different to the slower cooling rates. At 60 and  
323  $240^{\circ}\text{C h}^{-1}$   $CT_{\text{MIN}}$  was significantly lower relative to  $3^{\circ}\text{C h}^{-1}$  for *M. citrina* and *E. rubra* (Table 2,  
324 S5). For *M. citrina*, the values shifted depending on cooling rate, but with no clear pattern (Fig.  
325 3a). In contrast, *E. rubra* had stable  $CT_{\text{MIN}}$  values for 3, 6, and  $15^{\circ}\text{C h}^{-1}$  and more negative  
326 values as cooling rate increased to 30, 60, and  $240^{\circ}\text{C h}^{-1}$  (Table 2, S5, Fig. 3a).  $CT_{\text{MIN}}$  for *W.  
327 ceracea* was similar across most cooling rates and was only significantly different from when  
328 the cooling rate was  $30^{\circ}\text{C h}^{-1}$  (Table 2, S5). Variation in  $CT_{\text{MIN}}$  was independent of the initial  
329  $F_{\text{V}}/F_{\text{M}}$  of leaves.

330  $CT_{\text{MAX}}$  is typically measured with a heating rate of  $60^{\circ}\text{C h}^{-1}$ , so this was used as a  
331 reference against which all other heating rates were compared.  $CT_{\text{MAX}}$  was highly dependent on  
332 heating rate, where rates slower than  $60^{\circ}\text{C h}^{-1}$  produced significantly lower  $CT_{\text{MAX}}$  estimates,  
333 except for  $6^{\circ}\text{C h}^{-1}$ . Heating rates higher than  $60^{\circ}\text{C h}^{-1}$  resulted in higher  $CT_{\text{MAX}}$  estimates,  
334 significantly so for  $240^{\circ}\text{C h}^{-1}$  but not  $120^{\circ}\text{C h}^{-1}$  (Table 2, S6). However, stark species-specific  
335 responses were evident.  $CT_{\text{MAX}}$  in *M. citrina* was very low at heating rates of 6 and  $15^{\circ}\text{C h}^{-1}$  and  
336 increased significantly and consistently with faster heating rates: only 45 and  $60^{\circ}\text{C h}^{-1}$  yielded  
337 similar  $CT_{\text{MAX}}$  values (Table 2, S6, Fig. 3b). In contrast,  $CT_{\text{MAX}}$  in *E. rubra* was higher at the  
338 slowest rate (although the effect was marginal) compared to  $60^{\circ}\text{C h}^{-1}$  but significantly lower at  
339 30 and  $45^{\circ}\text{C h}^{-1}$  and not different from 120 and  $240^{\circ}\text{C h}^{-1}$  (Table 2, S6, Fig. 3b). Similarly,  
340 *W. ceracea* had significantly higher  $CT_{\text{MAX}}$  values at  $6^{\circ}\text{C h}^{-1}$ , but also at 120 and  $240^{\circ}\text{C h}^{-1}$ .  
341 Only 45 and  $60^{\circ}\text{C h}^{-1}$  produced  $CT_{\text{MAX}}$  values for *W. ceracea* that were not significantly

342 different (Table 2, S6, Fig. 3b). In all analyses except *E. rubra* individually,  $F_V/F_M$  had a  
343 significant positive relationship with  $CT_{MAX}$ .

344

345 ***Heating/cooling rate experiment: predicted thermal limits as a function of heating/cooling***  
346 ***rate***

347 We then modelled predicted  $CT_{MAX}$  and  $CT_{MIN}$  values against heating/cooling rate as a  
348 continuous variable using a quadratic function to visualise the interspecific differences in  
349 response to different heating/cooling rates when measuring thermal limits (Fig. 4a, b). The  
350 difference between 60 and 240°C h<sup>-1</sup> introduced extreme uncertainty in the predicted  $CT_{MIN}$  for  
351 *M. citrina*, so the 240°C h<sup>-1</sup> rate was removed from the visualisation. The shape of each species'  
352  $CT_{MAX}$  and  $CT_{MIN}$  response to heating/cooling rate were clearly distinct from one another and  
353 only *E. rubra* had a relatively stable predicted  $CT_{MAX}$  value across all measured heating/cooling  
354 rates. The variance tends to increase with faster heating/cooling rates for  $CT_{MIN}$ , but the pattern  
355 is less clear for  $CT_{MAX}$ .

356

357 **Discussion**

358 We sought to develop a reliable, high-throughput method for assessing thermal tolerance limits  
359 of the photosynthetic apparatus. Many methods are used for measuring plant thermal tolerance  
360 limits, but such variation has potential consequences for generating reasonable interpretations  
361 and interspecific comparisons. Often, the rationale behind a published method is unclear and the  
362 impacts of small methodological differences are difficult to assess (Geange *et al.* 2021). To  
363 address this, we have demonstrated a method for measuring both cold and heat tolerance limits  
364 of leaves using a thermoelectric plate and chlorophyll imaging fluorescence. In line with  
365 previous applications of this technique, we provide evidence for the effects of controllable  
366 experimental variables on estimates of  $CT_{MIN}$  and  $CT_{MAX}$ . We quantify the significant effects of  
367 measurement conditions and show that using a wet *vs* dry surface for measuring  $CT_{MIN}$  and that  
368 variation in heating/cooling rates leads to substantial differences in  $CT_{MIN}$  and  $CT_{MAX}$ . We  
369 aimed to develop a practical method that maximises informative value and minimises  
370 experimental noise among samples. In the case of heating/cooling rate, there is high species  
371 specificity. Below we outline potential mechanistic explanations for our findings along with  
372 testable hypotheses, and then propose best practices for measuring the thermal tolerance limits  
373 of leaves.

374

375

376 **Pros and cons of the  $T$ - $F_0$  Peltier plate-Maxi-Imaging fluorimeter method**

377 Measuring the temperature-dependent change in basal chlorophyll fluorescence is one of several  
378 potential methods that researchers can use to quantify the critical thermal limits of  
379 photosynthesis activation and photosynthetic apparatus stability (Ilík *et al.* 2003). The method  
380 that we present here offers improvements over earlier and alternative versions that use bulky  
381 water baths or freezing chambers, or smaller capacity Peltier plates (e.g., Schreiber and Berry  
382 1977; Braun *et al.* 2002; Knight and Ackerly 2002; Neuner and Pramsohler 2006), and adds  
383 several key features. The Peltier plate-Maxi-Imaging fluorimeter system is relatively compact  
384 and transportable for field applications when provided with a continuous power source. It offers  
385 precise temperature control ( $\pm 0.1^\circ\text{C}$  precision and  $\pm 1^\circ\text{C}$  tolerance) and high versatility by  
386 being programmable for both cooling and heating rapidly at set rates. It can be programmed for  
387 stepwise temperature treatments or non-linear temperature programs, or temperature shock  
388 treatments depending on the desired application. Furthermore, the  $T$ - $F_0$  curve allows for the  
389 calculation of other parameters (e.g., Knight and Ackerly 2002), including the temperatures at  
390 50% or 100% of relative  $F_0$  ( $T_{50}$  and  $T_{\max}$ , respectively) and ice nucleation temperatures ( $NT$ ) for  
391 cold tolerance assays if each leaf sample has a thermocouple attached to it (e.g., Briceño *et al.*  
392 2014). When using detached leaves or leaf discs, the potential throughput of the system is  
393 substantial (Fig. S1). The  $120 \times 90$  mm optimal imaging area on the Peltier plate can fit  $> 100$   
394 leaf discs or small leaf samples up to  $1 \text{ cm}^2$  or  $> 30$  samples that are up to  $2 \text{ cm}^2$  each, thus  
395 throughput is mostly constrained by sampling and setting up that many leaves.

396 As with any laboratory equipment, there are limitations to the Peltier plate-Maxi-  
397 Imaging fluorimeter system. Unlike freezing chambers, this system does not allow for whole-  
398 plant measurements. There is some software modification required for controlling the  
399 heating/cooling rates using the Peltier plate system, although newer temperature controllers and  
400 software revisions than those used here are now available. The Peltier plate-Maxi-Imaging  
401 fluorimeter system is a versatile phenotyping tool for thermal tolerance, ecophysiology, and  
402 photosynthesis research. Below, we discuss the results of testing the system with wet and dry  
403 filter paper as surfaces and the effects of heating/cooling rates.

404

405 **A dry surface avoids experimental artefacts**

406 Using wet filter paper as a surface for the leaf samples significantly reduced the apparent  
407 measured  $CT_{\min}$  but had no effect on  $CT_{\max}$ . Wet filter paper was initially tested to attempt to  
408 avoid leaf dehydration by providing a saturating atmosphere, preventing leaf evapotranspiration.  
409 In our cold tolerance assay, freezing of the water in the wet filter paper most likely began

410 propagating ice from outside the leaf into the apoplastic space, thereby freezing the apoplast in  
411 the leaf tissue at higher temperatures than leaves on the dry surface. When radiative frost occurs,  
412 air humidity condenses on the leaf surface, resulting in a wet leaf surface that may induce  
413 heterogenous extrinsic nucleation in natural frosts (Pearce 2001). Thus, the wet filter paper  
414 surface acted as an extrinsic ice nucleator and likely prevented the leaves from supercooling  
415 (Sakai and Larcher 1987; Pearce 2001; Larcher 2003). Our exploratory tests between wet and  
416 dry surfaces at different cooling rates demonstrated that on a dry filter paper surface, leaves  
417 appeared to supercool 2–4°C below those leaves on a wet surface. *NT* occurred earlier and at  
418 temperatures closer to  $CT_{MIN}$  on the wet surface and was more variable in comparison to leaves  
419 on a dry surface. Although this supercooling phenomenon requires further targeted investigation  
420 in future, our initial tests suggest that a wet surface induces earlier ice formation and  
421 propagation at warmer temperatures and hence reduces leaf supercooling capacity, and that  
422 supercooling capacity might be exacerbated by faster cooling rates.

423 The initial water status of leaf samples is still crucial, as water-stressed leaves can have  
424 compromised (Verslues *et al.* 2006) or even enhanced stress tolerance (Havaux 1992).  
425 Therefore, we recommend that detached leaves should be transported in a manner that maintains  
426 leaf water content after sampling (e.g., sealing leaves with plastic film wrap, using damp paper  
427 towel, or cut stems placed in water) so that leaves are either maintained at collection conditions  
428 or fully hydrated at the start of the thermal tolerance assay.

429

### 430 ***Maximising throughput without compromising results***

431 A wide range of heating/cooling rates have been used in previous studies of thermal limits to  
432 photosynthesis (Table S1). We have demonstrated that heating/cooling rate strongly influences  
433 both  $CT_{MIN}$  and  $CT_{MAX}$  values with varying magnitude and complex patterns for different  
434 species. Indeed, we saw such strong species-specific responses to different heating/cooling rates  
435 (particularly for heat) that if one were to measure the  $CT_{MAX}$  for three species measured at the  
436 same heating rate of  $45^{\circ}\text{C h}^{-1}$ , they would conclude that all the species have identical heat  
437 threshold temperatures, yet the same experiment conducted with a heating rate of  $6^{\circ}\text{C h}^{-1}$  and  
438  $240^{\circ}\text{C h}^{-1}$  would result in entirely different, and opposing, conclusions. For comparative studies  
439 that measure species with different leaf morphology, physiology, and biochemical constituents,  
440 it is crucial that we clarify and refine what physiological event(s) we aim to characterise with  
441 the  $T\text{-}F_0$  approach. From a practical standpoint, our aim was to identify the fastest  
442 heating/cooling rates that would allow repeatable, interpretable measures of  $T_{crit}$ .

443            Heating rates will determine the potential for activation and extent of the upregulation of  
444            physiological processes and protective mechanisms within the leaf when approaching thermal  
445            extremes (Bilger *et al.* 1984; Frolec *et al.* 2008). The rise in  $F_0$  during a measure of  $CT_{MAX}$   
446            indicates when photosynthetic activity is markedly reduced and thereafter the thylakoid  
447            membrane is disrupted (Havaux *et al.* 1988; Nauš *et al.* 1992). If leaf samples are heated only up  
448            to the temperature of the initial rise in  $F_0$ ,  $CT_{MAX}$ , and then cooled, it is possible that membrane  
449            disruption can be reversed (Yamane *et al.* 1997; Frolec *et al.* 2008). However, irreversible  
450            damage to PSII through physiological changes to the photosynthetic apparatus and then physical  
451            membrane separation (i.e., denaturation) is correlated with the continued rapid rise and maxima  
452            of  $F_0$  with sustained extreme temperatures (Terzaghi *et al.* 1989; Frolec *et al.* 2008).  
453            Specifically, the first peak in  $F_0$  shortly after  $CT_{MAX}$  and between 40–50°C is due to irreversible  
454            inactivation of PSII and the secondary  $F_0$  peak between 55–60°C originates from the denaturing  
455            of chlorophyll-containing protein complexes (Ilík *et al.* 2003). Leaves can reduce the  
456            photochemical and oxidative impairment induced by heat stress by thermal dissipation of  
457            excessive excitation energy to maintain PSII in an oxidative state, and by upregulating heat  
458            shock proteins and antioxidant activity (Allakhverdiev *et al.* 2008; Silva *et al.* 2010). Changes to  
459            the lipid composition of the thylakoid membrane reduces the fluidity of the membrane thereby  
460            being more stable at high temperatures (Allakhverdiev *et al.* 2008). The upregulation of these  
461            protective mechanisms of PSII can occur relatively quickly, sometimes < 1 h of heat stress  
462            (Havaux 1993), thus how protected the leaf is against PSII inactivation will depend on the  
463            heating rate.

464            For cold tolerance assays, cooling rates likely modify the dynamic and primary site of  
465            ice nucleation. Intrinsic ice nucleation may lead to ice formation in the xylem (Hacker and  
466            Neuner 2007), while extrinsic nucleation occurs at the leaf epidermis (Pearce and Ashworth  
467            1992). Rates of cooling may also influence supercooling capacity; usually faster cooling (within  
468            the range of this study) increases supercooling capacity (Gokhale 1965). Despite most freezing  
469            studies using cooling rates that are more reminiscent of natural freezing rates ( $\leq 5^{\circ}\text{C h}^{-1}$ ), we did  
470            not find a clear difference among  $CT_{MIN}$  values at cooling rates of 3, 6, and  $15^{\circ}\text{C h}^{-1}$ . We  
471            hypothesise that reducing the temperature relatively slowly (e.g.,  $\leq 15^{\circ}\text{C h}^{-1}$ ) could allow the  
472            cell to adjust osmotically and partially counterbalance the reduced water potential of the frozen  
473            apoplast restricting cell dehydration, which would be avoided at faster cooling speeds. Thus, the  
474            consideration for the freezing tolerance cooling rates becomes a question of what is the greatest  
475            cooling rate that allows more realistic osmotic adjustments within the leaf.

476 For *W. ceracea* and *E. rubra*, increasing temperature slowly ( $< 30^{\circ}\text{C h}^{-1}$ ) appears to  
477 allow time for induction of protective mechanisms such that slower heating rates result in higher  
478  $CT_{\text{MAX}}$  values. Conversely, changing temperature more quickly ( $30\text{--}60^{\circ}\text{C h}^{-1}$ ) prevents  
479 membranes from inducing heat-hardening or for antioxidants to be upregulated and take effect,  
480 such that measured heat tolerance limits is relatively stable at these heating rates. Our results  
481 indicate that beyond a rate of  $60^{\circ}\text{C h}^{-1}$ , the increase in  $F_0$  occurs more slowly than the  
482 temperature increase and the temperature of the leaf samples (as measured by thermocouples)  
483 also lags significantly behind the temperature of the Peltier plate, thus the  $CT_{\text{MAX}}$  may be  
484 overestimated (Fig. 3b). Hence, using the thermistor (plate) temperature will overestimate the  
485 temperature of the leaf, and therefore, its tolerance limit. Furthermore, the faster that the plate  
486 temperature is changed, the more potential variation among leaf temperatures. We acknowledge  
487 that the method could be improved by using individual thermocouples for each leaf sample,  
488 particularly for cold tolerance to measure ice nucleation temperature ( $NT$ ), however, we have  
489 verified that there is minimal variation ( $\pm 1^{\circ}\text{C}$ ) across the Peltier plate surface.

490 The species specificity of the heating rate dependence of  $CT_{\text{MAX}}$  was striking,  
491 particularly in the case of *M. citrina*. A slow heating rate of  $6^{\circ}\text{C h}^{-1}$  results in a very low  
492 estimate for  $CT_{\text{MAX}}$  of only  $36^{\circ}\text{C}$ , which suggests that the heat tolerance of this species is poor,  
493 yet at heating rates  $\geq 30^{\circ}\text{C h}^{-1}$ , this species is apparently as or more heat tolerant than the other  
494 species. Slow heating rates mean that the leaves are slow to reach more stressful temperatures,  
495 but also that they are held at these temperatures for longer periods of time. We hypothesise that  
496 the lower heat tolerance limit at slow heating rates could be due to leaf water being tightly  
497 bound and preventing cooling via transpiration or the heated leaf oils being unable to volatilise,  
498 thereby destabilising membranes and effectively ‘slow-cooking’ the leaf. For this species, the  
499 higher heating rates are therefore likely more indicative of photosynthetic thermal tolerance  
500 limits.

501 The  $T-F_0$  method is a rapid measurement compared to other  $F_{\text{V}}/F_{\text{M}}$ -based assessments of  
502 thermal tolerance. Determining the temperature at which 50% of the potential thermal damage  
503 (lethal temperature) to the plant tissue occurs ( $LT_{50}$ ) is a common but very time-consuming  
504 technique that also requires more plant material. Different individual leaves are heated/cooled to  
505 and held at set temperatures for 1-3 h, and then  $F_{\text{V}}/F_{\text{M}}$  is measured over 1-24 h post-thermal  
506 exposure to determine the point of irreversible damage. We note that  $F_0$  can be affected by leaf  
507 properties including the efficiency of PSII, the leaf chlorophyll content and ratios, and leaf  
508 thickness, which may affect thermal tolerance estimates more than those measured using  $F_{\text{V}}/F_{\text{M}}$ .  
509 Therefore, to better understand what occurs within a leaf during exposure to thermal extremes, it

510 would be valuable to characterise the  $T$ - $F_0$  curve and identify the  $CT_{\text{MIN}}$  and  $CT_{\text{MAX}}$  values for a  
511 plant. One could then heat/cool and hold leaf samples at these threshold temperatures for a set  
512 time, then measure  $F_v/F_M$  with the same Maxi-Imaging fluorescence system to examine  
513 potential recovery from exposure to damaging temperatures (e.g., Buchner *et al.* 2015). Then,  
514 one could investigate the correlation between  $CT$  and  $LT$  metrics and determine the extent and  
515 reversibility of damage. A more complete micro-scale understanding of thermal tolerance  
516 responses and species specificity would be enhanced by exploring tissue biochemistry, the  
517 regulation of heat shock proteins, and gene expression at thermal extremes (Geange *et al.* 2021).  
518 At the macro end of the scale, remote sensing tools allows landscape scale estimations of  
519 photosynthetic tolerance to heating using the Photochemical Reflectance Index (PRI), which  
520 strongly relates to stress changes in photosynthetic machinery (Sukhova and Sukhov 2018;  
521 Yudina *et al.* 2020). Comparative studies on the accuracy and precision of different micro- and  
522 macro-scale techniques for estimating thermal tolerance of plants will be necessary for  
523 maximising agricultural and ecological monitoring efforts.

524

#### 525 ***Towards standardised approaches for comparative thermal tolerance research***

526 There will never be a perfect one-size-fits-all method for comparative measures of plant  
527 photosynthetic thermal tolerance, but our exploration of method variation we find there is a  
528 reasonable set of conditions that will fit most. We advocate that researchers use well-hydrated  
529 leaves (unless hydration status is an element of their experiment) and dry surface for these  
530 measures. Doing so allows easy comparison across experiments and gives a more indicative  
531 measure of the lowest potential  $CT_{\text{MIN}}$ .

532 We sought the maximum heating/cooling rate that was repeatable and reliable. Our  
533 results suggest that there is a point beyond which temperatures are changed too quickly and the  
534  $T_{\text{crit}}$  value is exaggerated due to the change in  $F_0$  lagging the change in leaf temperature,  
535 especially in heat tolerance limit assays. For an experiment on a single or few species, pilot  
536 studies on the effects of heating/cooling rates are advisable. For broad interspecific studies,  
537 particularly in natural systems where other variables such as thermal history and the  
538 environment cannot be controlled, using a common rate for heating and for cooling is the only  
539 feasible approach. For such comparative work, we recommend a heating rate of not less than  
540  $30^{\circ}\text{C h}^{-1}$  (up to  $60^{\circ}\text{C h}^{-1}$  to avoid any potential heat hardening) for  $CT_{\text{MAX}}$  and a cooling rate at  
541 or below  $15^{\circ}\text{C h}^{-1}$  for  $CT_{\text{MIN}}$ . We recognise that this is a slower heating rate than often used for  
542  $CT_{\text{MAX}}$  and a faster than usual cooling rate for  $CT_{\text{MIN}}$ . However, we found that the  $15^{\circ}\text{C h}^{-1}$  rate  
543 was not significantly different to slower rates for  $CT_{\text{MIN}}$  and thus represents the most efficient

544 rate that could yield results reflective of natural scenarios. For  $CT_{MAX}$ , we argue that the 30–  
545  $60^{\circ}\text{C h}^{-1}$  rates enable physiological mechanisms that would normally provide some thermal  
546 protection to the photosystem and cell membranes to be induced, without lag exaggerating  
547  $CT_{MAX}$ , and may therefore be a more realistic or relevant measurement of thermal tolerance than  
548 that provided by faster rates. These rates remain practical for achieving high throughput,  
549 especially with sample sizes that can be accommodated by large Peltier plates combined with  
550 the multi-sample imaging of Maxi-Imaging fluorimeters.

551 Clearly, any experimental thermal tolerance assay cannot perfectly mirror the conditions  
552 of a natural extreme thermal event. Rates of heating and cooling of plant tissues in nature are  
553 non-linear, not sustained, and strongly mediated by external conditions such as wind, solar  
554 radiation, season, and elevation (Sakai and Larcher 1987; Leuning and Cremer 1988; Vogel  
555 2009). The researcher must always remain appreciative of how extrinsic factors could affect  
556 these values and interpretations thereof for their study system. However,  $T-F_0$  curves and  
557 derived  $T_{crit}$  values can indicate what the *potential* thermal limits of leaves are, under absolute  
558 conditions. The method provides power for comparative research, and also ample opportunity to  
559 explore the underlying mechanisms of species level differentiation. Moving toward a deeper  
560 understanding of the physiological processes conferring thermal tolerance is crucial in the  
561 changing climate where extreme weather events are increasing in frequency and intensity  
562 (Buckley and Huey 2016; Harris *et al.* 2018).

563

#### 564 **Conclusions**

565 The Peltier plate-Maxi-Imaging fluorimeter system described and tested here allows relatively  
566 high-throughput measurement of  $T-F_0$  and the critical thermal limits to inactivation of  
567 photosynthesis. This system offers great flexibility and substantially expands on previous  
568 versions. We have demonstrated that use of wet *vs* dry surface can significantly affect the  $CT_{MIN}$   
569 estimate, but not  $CT_{MAX}$ , and that heating/cooling rates have strong species-specific effects on  
570 both  $CT_{MIN}$  and  $CT_{MAX}$ . Awareness of the physiological processes that underlie the rapid rise in  
571  $F_0$  and consideration of interspecific differences in leaf physiology and biochemistry are  
572 essential for making effective choices in the rate of heating or cooling leaf samples. We  
573 recommend the use of parameters that maximise repeatability and efficiency of the  
574 measurements without introducing artefacts of heating/cooling rate. As plants around the world  
575 are exposed to more thermal extremes by the effects of climate change, versatile  
576 ecophysiological tools such as this Peltier plate-Maxi-Imaging fluorimeter system will be  
577 valuable for generating new insights in plant responses and thermal tolerance limits.

578 **Conflicts of Interest**

579 The authors declare no conflicts of interest.

580

581 **Acknowledgements**

582 We sincerely thank Ya Zhang for modifying the LabVIEW software for heating/cooling rate  
583 control, ANU plant services staff for maintaining glasshouse plants, and Jack Egerton and ANU  
584 workshop staff for technical support. We thank three anonymous reviewers and Loeske Kruuk  
585 for their constructive feedback on earlier versions of this manuscript. This research was  
586 supported by the Australian Research Council (DP170101681).

587

588 **Author contribution statement**

589 PAA, KMG, AAC, and ABN designed the experiments. PAA, KMG, AAC performed the  
590 experiments and collected the data. PAA curated the data and performed the data analyses and  
591 visualisation. PAA, VFB, LAB, and ABN interpreted the results and wrote the manuscript with  
592 input from all authors.

593

594 **Supplemental material**

595 The following supplemental materials are available.

596 **Supplemental Table S1:** Samples of heating/cooling rate variation from the literature.

597 **Supplemental Table S2:** Mean values for  $CT_{\text{MIN}}$ ,  $CT_{\text{MAX}}$ , and  $F_V/F_M$  for each species and  
598 experimental condition.

599 **Supplemental Table S3:** Full statistical reporting for effects of wet vs dry surface for  $CT_{\text{MIN}}$   
600 and  $CT_{\text{MAX}}$ .

601 **Supplemental Table S4:** Full statistical reporting for effects of wet vs dry surface combined  
602 with heating/cooling rate on  $CT_{\text{MIN}}$ .

603 **Supplemental Table S5:** Full statistical reporting for effects of heating/cooling rate for  $CT_{\text{MIN}}$ .

604 **Supplemental Table S6:** Full statistical reporting for effects of heating/cooling rate for  $CT_{\text{MAX}}$ .

605 **Supplemental Figure S1:** Various experimental applications of the Peltier plate and  
606 chlorophyll fluorescence Maxi-Imaging-PAM system.

607 **Supplemental Figure S2:** Effects of wet vs dry surface combined with cooling rate on  $CT_{\text{MIN}}$   
608 and  $NT$ .

609 **References**

610 Allakhverdiev, SI, Kreslavski, VD, Klimov, VV, Los, DA, Carpentier, R, Mohanty, P (2008)  
611 Heat stress: an overview of molecular responses in photosynthesis. *Photosynthesis*  
612 *Research* **98**, 541-550.

613 Baker, NR (2008) Chlorophyll fluorescence: a probe of photosynthesis in vivo. *Annual Review*  
614 *of Plant Biology* **59**, 89-113.

615 Berry, J, Björkman, O (1980) Photosynthetic response and adaptation to temperature in higher  
616 plants. *Annual Review of Plant Physiology* **31**, 491-543.

617 Bilger, H-W, Schreiber, U, Lange, OL (1984) Determination of leaf heat resistance:  
618 comparative investigation of chlorophyll fluorescence changes and tissue necrosis  
619 methods. *Oecologia* **63**, 256-262.

620 Bita, CE, Gerats, T (2013) Plant tolerance to high temperature in a changing environment:  
621 scientific fundamentals and production of heat stress-tolerant crops. *Frontiers in Plant*  
622 *Science* **4**, 273.

623 Braun, V, Buchner, O, Neuner, G (2002) Thermotolerance of photosystem 2 of three alpine  
624 plant species under field conditions. *Photosynthetica* **40**, 587-595.

625 Briantais, J-M, Dacosta, J, Goulas, Y, Ducruet, J-M, Moya, I (1996) Heat stress induces in  
626 leaves an increase of the minimum level of chlorophyll fluorescence,  $F_0$ : A time-  
627 resolved analysis. *Photosynthesis Research* **48**, 189-196.

628 Briceño, VF, Harris-Pascal, D, Nicotra, AB, Williams, E, Ball, MC (2014) Variation in snow  
629 cover drives differences in frost resistance in seedlings of the alpine herb *Aciphylla*  
630 *glacialis*. *Environmental and Experimental Botany* **106**, 174-181.

631 Buchner, O, Neuner, G (2009) A low-temperature freezing system to study the effects of  
632 temperatures to  $-70^{\circ}\text{C}$  on trees in situ. *Tree Physiology* **29**, 313-320.

633 Buchner, O, Stoll, M, Karadar, M, Kranner, I, Neuner, G (2015) Application of heat stress in  
634 situ demonstrates a protective role of irradiation on photosynthetic performance in alpine  
635 plants. *Plant, Cell & Environment* **38**, 812-826.

636 Buckley, LB, Huey, RB (2016) How extreme temperatures impact organisms and the evolution  
637 of their thermal tolerance. *Integrative and Comparative Biology* **56**, 98-109.

638 Frolec, J, Ilík, P, Krchňák, P, Sušila, P, Nauš, J (2008) Irreversible changes in barley leaf  
639 chlorophyll fluorescence detected by the fluorescence temperature curve in a linear  
640 heating/cooling regime. *Photosynthetica* **46**, 537-546.

641 Geange, SR, Arnold, PA, Catling, AA, Coast, O, Cook, AM, Gowland, KM, Leigh, A,  
642 Notarnicola, RF, Posch, BC, Venn, SE, Zhu, L, Nicotra, AB (2021) The thermal  
643 tolerance of photosynthetic tissues: a global systematic review and agenda for future  
644 research. *New Phytologist* 10.1111/nph.17052.

645 Goh, C-H, Ko, S-M, Koh, S, Kim, Y-J, Bae, H-J (2012) Photosynthesis and environments:  
646 photoinhibition and repair mechanisms in plants. *Journal of Plant Biology* **55**, 93-101.

647 Gokhale, NR (1965) Dependence of freezing temperature of supercooled water drops on rate of  
648 cooling. *Journal of the Atmospheric Sciences* **22**, 212-216.

649 Goraya, GK, Kaur, B, Asthir, B, Bala, S, Kaur, G, Farooq, M (2017) Rapid injuries of high  
650 temperature in plants. *Journal of Plant Biology* **60**, 298-305.

651 Hacker, J, Neuner, G (2007) Ice propagation in plants visualized at the tissue level by infrared  
652 differential thermal analysis (IDTA). *Tree Physiology* **27**, 1661-1670.

653 Harrell, FEJ (2019) 'Hmisc: Harrell Miscellaneous.' [https://CRAN.R-  
654 project.org/package=Hmisc](https://CRAN.R-project.org/package=Hmisc)

655 Harris, RMB, Beaumont, LJ, Vance, TR, Tozer, CR, Remenyi, TA, Perkins-Kirkpatrick, SE,  
656 Mitchell, PJ, Nicotra, AB, McGregor, S, Andrew, NR, Letnic, M, Kearney, MR,  
657 Wernberg, T, Hutley, LB, Chambers, LE, Fletcher, MS, Keatley, MR, Woodward, CA,  
658 Williamson, G, Duke, NC, Bowman, DMJS (2018) Biological responses to the press and  
659 pulse of climate trends and extreme events. *Nature Climate Change* **8**, 579-587.

660 Havaux, M (1992) Stress tolerance of photosystem II *in vivo*. *Plant Physiology* **100**, 424-432.

661 Havaux, M (1993) Rapid photosynthetic adaptation to heat stress triggered in potato leaves by  
662 moderately elevated temperatures. *Plant, Cell & Environment* **16**, 461-467.

663 Havaux, M, Ernez, M, Lannoye, R (1988) Correlation between heat tolerance and drought  
664 tolerance in cereals demonstrated by rapid chlorophyll fluorescence tests. *Journal of*  
665 *Plant Physiology* **133**, 555-560.

666 Hüve, K, Bichele, I, Tobias, M, Niinemets, Ü (2006) Heat sensitivity of photosynthetic electron  
667 transport varies during the day due to changes in sugars and osmotic potential. *Plant,*  
668 *Cell & Environment* **29**, 212-228.

669 Ilík, P, Kouřil, R, Kruk, J, Myśliwa-Kurdziel, B, Popelková, H, Strzałka, K, Nauš, J (2003)  
670 Origin of chlorophyll fluorescence in plants at 55–75°C. *Photochemistry and*  
671 *Photobiology* **77**, 68-76.

672 IPCC (2018) Global Warming of 1.5° C: An IPCC Special Report on the Impacts of Global  
673 Warming of 1.5° C Above Pre-industrial Levels and Related Global Greenhouse Gas  
674 Emission Pathways, in the Context of Strengthening the Global Response to the Threat  
675 of Climate Change, Sustainable Development, and Efforts to Eradicate Poverty. Geneva,  
676 Switzerland. Available at <https://www.ipcc.ch/sr15/>.

677 Janion-Scheepers, C, Phillips, L, Sgrò, CM, Duffy, GA, Hallas, R, Chown, SL (2018) Basal  
678 resistance enhances warming tolerance of alien over indigenous species across latitude.  
679 *Proceedings of the National Academy of Sciences* **115**, 145-150.

680 Knight, CA, Ackerly, DD (2002) An ecological and evolutionary analysis of photosynthetic  
681 thermotolerance using the temperature-dependent increase in fluorescence. *Oecologia*  
682 **130**, 505-514.

683 Larcher, W (2003) 'Physiological plant ecology: ecophysiology and stress physiology of  
684 functional group.' (Springer-Verlag: Berlin, Germany)

685 Leigh, A, Sevanto, S, Ball, MC, Close, JD, Ellsworth, DS, Knight, CA, Nicotra, AB, Vogel, S  
686 (2012) Do thick leaves avoid thermal damage in critically low wind speeds? *New*  
687 *Phytologist* **194**, 477-487.

688 Leuning, R, Cremer, KW (1988) Leaf temperatures during radiation frost Part I. Observations.  
689 *Agricultural and Forest Meteorology* **42**, 121-133.

690 Logan, BA, Adams, WW, Demmig-Adams, B (2007) Avoiding common pitfalls of chlorophyll  
691 fluorescence analysis under field conditions. *Functional Plant Biology* **34**, 853-859.

692 Mathur, S, Agrawal, D, Jajoo, A (2014) Photosynthesis: response to high temperature stress.  
693 *Journal of Photochemistry and Photobiology B: Biology* **137**, 116-126.

694 Muggeo, VMR (2017) Interval estimation for the breakpoint in segmented regression: a  
695 smoothed score-based approach. *Australian & New Zealand Journal of Statistics* **59**,  
696 311-322.

697 Murchie, EH, Lawson, T (2013) Chlorophyll fluorescence analysis: a guide to good practice and  
698 understanding some new applications. *Journal of Experimental Botany* **64**, 3983-3998.

699 Nauš, J, Kuropatwa, R, Klinkovský, T, Ilík, P, Lattová, J, Pavlová, Z (1992) Heat injury of  
700 barley leaves detected by the chlorophyll fluorescence temperature curve. *Biochimica et  
701 Biophysica Acta (BBA) - Bioenergetics* **1101**, 359-362.

702 Neuner, G, Pramsohler, M (2006) Freezing and high temperature thresholds of photosystem 2  
703 compared to ice nucleation, frost and heat damage in evergreen subalpine plants.  
704 *Physiologia Plantarum* **126**, 196-204.

705 O'Sullivan, OS, Heskel, MA, Reich, PB, Tjoelker, MG, Weerasinghe, LK, Penillard, A, Zhu, L,  
706 Egerton, JG, Bloomfield, KJ, Creek, D, Bahar, NHA, Griffin, KL, Hurry, V, Meir, P,  
707 Turnbull, MH, Atkin, OK (2017) Thermal limits of leaf metabolism across biomes.  
708 *Global Change Biology* **23**, 209-223.

709 O'Sullivan, OS, Weerasinghe, KWLK, Evans, JR, Egerton, JG, Tjoelker, MG, Atkin, OK  
710 (2013) High-resolution temperature responses of leaf respiration in snow gum  
711 (*Eucalyptus pauciflora*) reveal high-temperature limits to respiratory function. *Plant,  
712 Cell & Environment* **36**, 1268-1284.

713 Pearce, RS (2001) Plant freezing and damage. *Annals of Botany* **87**, 417-424.

714 Pearce, RS, Ashworth, EN (1992) Cell shape and localisation of ice in leaves of overwintering  
715 wheat during frost stress in the field. *Planta* **188**, 324-331.

716 Potvin, C (1985) Effect of leaf detachment on chlorophyll fluorescence during chilling  
717 experiments. *Plant Physiology* **78**, 883-886.

718 R Core Team (2020) 'R: A language and environment for statistical computing.' (R Foundation  
719 for Statistical Computing: Vienna, Austria)

720 Sakai, A, Larcher, W (1987) 'Frost survival of plants: responses and adaptation to freezing  
721 stress.' (Springer-Verlag: Berlin, Germany)

722 Schreiber, U, Berry, JA (1977) Heat-induced changes of chlorophyll fluorescence in intact  
723 leaves correlated with damage of the photosynthetic apparatus. *Planta* **136**, 233-238.

724 Schreiber, U, Hormann, H, Neubauer, C, Klughammer, C (1995) Assessment of photosystem II  
725 photochemical quantum yield by chlorophyll fluorescence quenching analysis.  
726 *Functional Plant Biology* **22**, 209-220.

727 Silva, EN, Ferreira-Silva, SL, Fontenele, AdV, Ribeiro, RV, Viégas, RA, Silveira, JAG (2010)  
728 Photosynthetic changes and protective mechanisms against oxidative damage subjected  
729 to isolated and combined drought and heat stresses in *Jatropha curcas* plants. *Journal of*  
730 *Plant Physiology* **167**, 1157-1164.

731 Sinclair, BJ, Marshall, KE, Sewell, MA, Levesque, DL, Willett, CS, Slotsbo, S, Dong, Y,  
732 Harley, CDG, Marshall, DJ, Helmuth, BS, Huey, RB (2016) Can we predict ectotherm  
733 responses to climate change using thermal performance curves and body temperatures?  
734 *Ecology Letters* **19**, 1372-1385.

735 Smillie, RM, Nott, R, Hetherington, SE, Öquist, G (1987) Chilling injury and recovery in  
736 detached and attached leaves measured by chlorophyll fluorescence. *Physiologia*  
737 *Plantarum* **69**, 419-428.

738 Sukhov, V, Gaspirovich, V, Mysyagin, S, Vodeneev, V (2017) High-temperature tolerance of  
739 photosynthesis can be linked to local electrical responses in leaves of pea. *Frontiers in*  
740 *Physiology* **8**, 763.

741 Sukhova, E, Sukhov, V (2018) Connection of the photochemical reflectance index (PRI) with  
742 the photosystem II quantum yield and nonphotochemical quenching can be dependent on  
743 variations of photosynthetic parameters among investigated plants: a meta-analysis.  
744 *Remote Sensing* **10**, 771.

745 Sung, D-Y, Kaplan, F, Lee, K-J, Guy, CL (2003) Acquired tolerance to temperature extremes.  
746 *Trends in Plant Science* **8**, 179-187.

747 Terzaghi, WB, Fork, DC, Berry, JA, Field, CB (1989) Low and high temperature limits to PSII.  
748 *Plant Physiology* **91**, 1494-1500.

749 Verslues, PE, Agarwal, M, Katiyar-Agarwal, S, Zhu, J, Zhu, J-K (2006) Methods and concepts  
750 in quantifying resistance to drought, salt and freezing, abiotic stresses that affect plant  
751 water status. *The Plant Journal* **45**, 523-539.

752 Vogel, S (2009) Leaves in the lowest and highest winds: temperature, force and shape. *New*  
753 *Phytologist* **183**, 13-26.

754 Yamane, Y, Kashino, Y, Koike, H, Satoh, K (1997) Increases in the fluorescence  $F_o$  level and  
755 reversible inhibition of Photosystem II reaction center by high-temperature treatments in  
756 higher plants. *Photosynthesis Research* **52**, 57-64.

757 Yudina, L, Sukhova, E, Gromova, E, Nerush, V, Vodeneev, V, Sukhov, V (2020) A light-  
758 induced decrease in the photochemical reflectance index (PRI) can be used to estimate  
759 the energy-dependent component of non-photochemical quenching under heat stress and  
760 soil drought in pea, wheat, and pumpkin. *Photosynthesis Research* **146**, 175-187.

761 Zhu, L, Bloomfield, KJ, Hocart, CH, Egerton, JJG, O'Sullivan, OS, Penillard, A, Weerasinghe,  
762 LK, Atkin, OK (2018) Plasticity of photosynthetic heat tolerance in plants adapted to  
763 thermally contrasting biomes. *Plant, Cell & Environment* **41**, 1251-1262.

764 Zinn, KE, Tunc-Ozdemir, M, Harper, JF (2010) Temperature stress and plant sexual  
765 reproduction: uncovering the weakest links. *Journal of Experimental Botany* **61**, 1959-  
766 1968.

767

768

769 **Tables**

770

771 **Table 1.** Summary of analyses of all species and species-specific effects of wet vs dry filter  
772 paper surface on  $CT_{\text{MIN}}$  and  $CT_{\text{MAX}}$ .

Response: $CT_{\text{MIN}}$	All species	<i>W. ceracea</i>	<i>M. citrina</i>	<i>E. rubra</i>
Fixed effects	Estimate	Estimate	Estimate	Estimate
Dry surface / <i>E. rubra</i> (intercept)	<b>-18.36*</b>	Intercept: -5.71	Intercept: <b>-20.36*</b>	Intercept: <b>-31.26**</b>
Wet surface	<b>3.81***</b>	<b>3.92***</b>	<b>2.98**</b>	<b>3.99***</b>
$F_V/F_M$	6.19	-9.89	4.72	23.54
<i>M. citrina</i>	<b>-3.50***</b>	--	--	--
<i>W. ceracea</i>	-0.42	--	--	--
$R^2$	0.464	0.288	0.374	0.527

Response: $CT_{\text{MAX}}$	All species	<i>W. ceracea</i>	<i>M. citrina</i>	<i>Q. phellos</i>
Fixed effects	Estimate	Estimate	Estimate	Estimate
Dry surface / <i>M. citrina</i> (intercept)	<b>32.76***</b>	Intercept: 6.90	Intercept: <b>36.31*</b>	Intercept: <b>47.34***</b>
Wet surface	-0.55	-1.47	0.32	-0.63
$F_V/F_M$	18.20	<b>46.02*</b>	13.16	2.32
<i>Q. phellos</i>	<b>2.01**</b>	--	--	--
<i>W. ceracea</i>	<b>-4.47***</b>	--	--	--
$R^2$	0.593	0.213	0.028	0.041

773 *Bold* indicates significance at  $p < 0.05$ , \*:  $p < 0.05$ , \*\*:  $p < 0.01$ , \*\*\*:  $p < 0.001$ . Intercepts marked as

774 significant are different from zero. Full statistical reporting is provided in Table S3.

775

776 **Table 2:** Summary of analyses of all species and species-specific effects of variable temperature  
 777 heating/cooling rate on  $CT_{\text{MIN}}$  and  $CT_{\text{MAX}}$ .

Response: $CT_{\text{MIN}}$	All species	<i>W. ceracea</i>	<i>M. citrina</i>	<i>E. rubra</i>
Fixed effects	Estimate	Estimate	Estimate	Estimate
Cooling rate = $3^{\circ}\text{C h}^{-1}$ / <i>E. rubra</i> (Intercept)	<b>-11.38***</b>	Intercept: <b>-40.89**</b>	Intercept: <b>-16.82***</b>	Intercept: <b>-11.58**</b>
Cooling rate = $6^{\circ}\text{C h}^{-1}$	-0.33	0.62	<b>-1.81*</b>	-0.15
Cooling rate = $15^{\circ}\text{C h}^{-1}$	-0.32	-0.12	-0.80	-0.10
Cooling rate = $30^{\circ}\text{C h}^{-1}$	0.75	<b>1.67**</b>	0.91	-0.74
Cooling rate = $60^{\circ}\text{C h}^{-1}$	<b>-1.34**</b>	0.75	<b>-3.51***</b>	<b>-2.47***</b>
Cooling rate = $240^{\circ}\text{C h}^{-1}$	-0.80	0.70	<b>-1.74*</b>	<b>-1.90**</b>
$F_V/F_M$	-0.89	32.04	4.66	0.12
<i>M. citrina</i>	<b>-2.18***</b>	--	--	--
<i>W. ceracea</i>	<b>-1.53**</b>	--	--	--
Marginal R <sup>2</sup>	0.230	0.126	0.332	0.220
Response: $CT_{\text{MAX}}$	All species	<i>W. ceracea</i>	<i>M. citrina</i>	<i>E. rubra</i>
Fixed effects	Estimate	Estimate	Estimate	Estimate
Heating rate = $60^{\circ}\text{C h}^{-1}$ / <i>E. rubra</i> (Intercept)	<b>27.79***</b>	Intercept: 14.87	Intercept: <b>27.79***</b>	Intercept: <b>41.75*</b>
Heating rate = $6^{\circ}\text{C h}^{-1}$	-0.68	<b>1.60*</b>	<b>-7.71***</b>	1.38
Heating rate = $15^{\circ}\text{C h}^{-1}$	<b>2.43***</b>	<b>-2.00**</b>	<b>-4.68***</b>	-1.40
Heating rate = $30^{\circ}\text{C h}^{-1}$	<b>-1.74**</b>	<b>-2.11***</b>	<b>-2.10**</b>	<b>-1.31*</b>
Heating rate = $45^{\circ}\text{C h}^{-1}$	<b>-1.48**</b>	-0.72	-0.95	<b>-2.68***</b>
Heating rate = $120^{\circ}\text{C h}^{-1}$	1.00	<b>1.78**</b>	<b>2.24*</b>	-0.45
Heating rate = $240^{\circ}\text{C h}^{-1}$	<b>2.03***</b>	<b>2.78***</b>	<b>3.76***</b>	-0.13
$F_V/F_M$	<b>23.79***</b>	<b>38.48***</b>	<b>21.98**</b>	5.15
<i>M. citrina</i>	<b>-1.30***</b>	--	--	--
<i>W. ceracea</i>	<b>-1.24**</b>	--	--	--
Marginal R <sup>2</sup>	0.429	0.619	0.863	0.319

778 *Bold* indicates significance at  $p < 0.05$ , \*:  $p < 0.05$ , \*\*:  $p < 0.01$ , \*\*\*:  $p < 0.001$ . Intercepts marked as  
 779 significant are different from zero. Full statistical reporting is provided in Tables S5 and S6.

780

781 **Figures**

782 **Fig. 1.** Experimental system for measuring thermal tolerance limits and representative  
783 temperature-dependent chlorophyll fluorescence curves ( $T$ - $F_0$ ). (a) The Peltier plate-Maxi-  
784 Imaging fluorimeter setup for measuring leaf thermal tolerance limits. (b) Representative  $T$ - $F_0$   
785 curve for  $CT_{\text{MIN}}$  (inflection point is the  $T_{\text{crit}}$ ) where leaf sample temperature (°C) decreases to a  
786 point below freezing where the leaf rapidly emits more fluorescence ( $F_0$ , relative units),  
787 indicating the onset of photosynthetic inactivation and freeze dehydration. (c) Representative  $T$ -  
788  $F_0$  curve for  $CT_{\text{MAX}}$  (inflection point is the  $T_{\text{crit}}$ ) where leaf sample temperature (°C) increases  
789 beyond tolerance thresholds where the leaf rapidly emits more fluorescence ( $F_0$ , relative units),  
790 indicating the onset of photosynthetic inactivation and potential damage. The example  $T$ - $F_0$   
791 curve for (b)  $CT_{\text{MIN}}$  is derived from a leaf sample on dry filter paper cooled at 15°C h<sup>-1</sup> and for  
792 (c)  $CT_{\text{MAX}}$  is derived from a leaf sample on dry filter paper heated at 30°C h<sup>-1</sup>. The direction of  
793 arrows below the  $x$ -axes indicates the direction of temperature change.

794

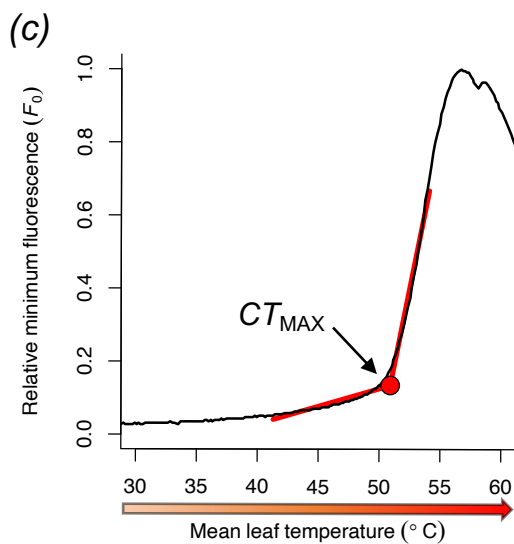
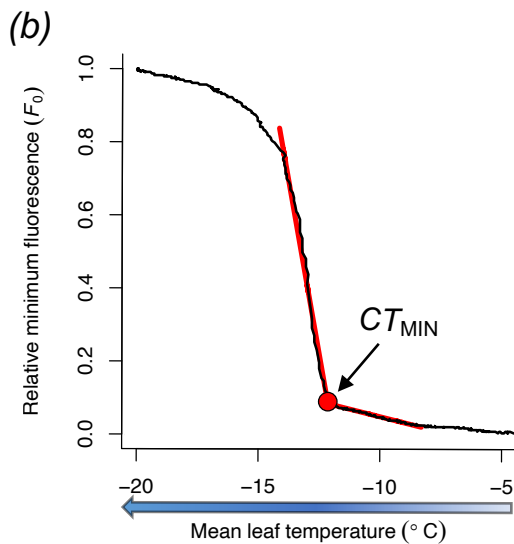
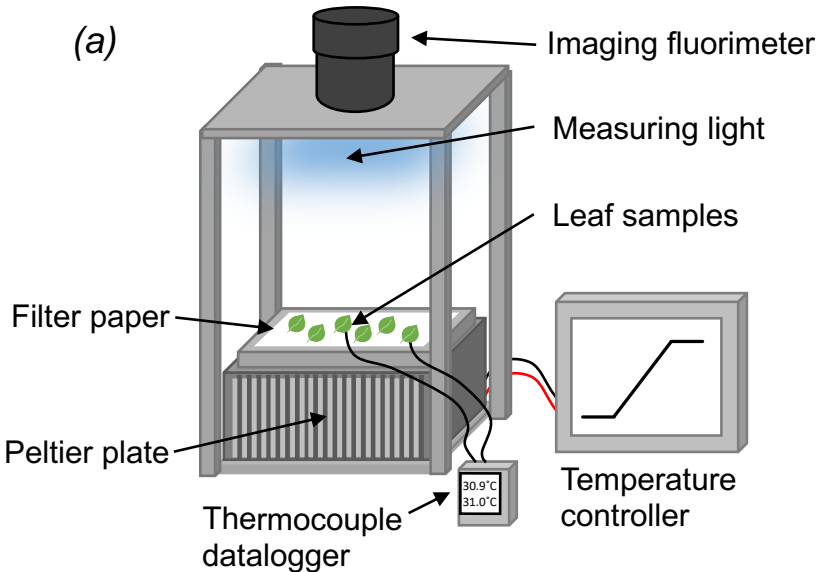
795 **Fig. 2.** The effect of varying surfaces (dry *vs* wet filter paper) on the  $CT_{\text{MIN}}$  and  $CT_{\text{MAX}}$   
796 estimates (°C) from basal chlorophyll fluorescence ( $F_0$ , relative units) of leaves. We tested how  
797 (a)  $CT_{\text{MIN}}$  and (b)  $CT_{\text{MAX}}$  estimates of leaves from four plant species under standard dry  
798 conditions (dry filter paper surface) differed from wet conditions (wet filter paper surface). All  
799 estimated were obtained using a standard heating/cooling rate of 60°C h<sup>-1</sup>. Data points are means  
800 and 95% CIs that overlay raw data ( $n = 12$ –25 per treatment  $\times$  species combination).

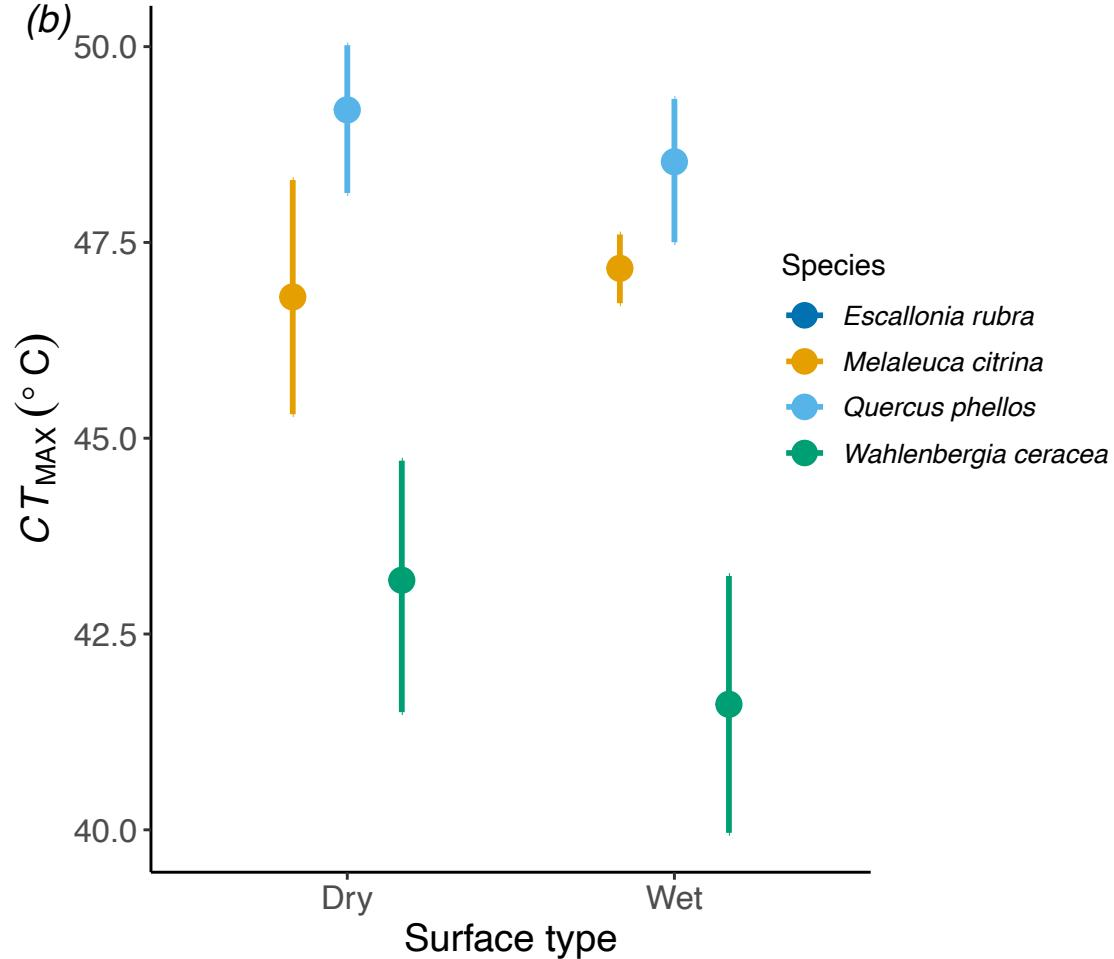
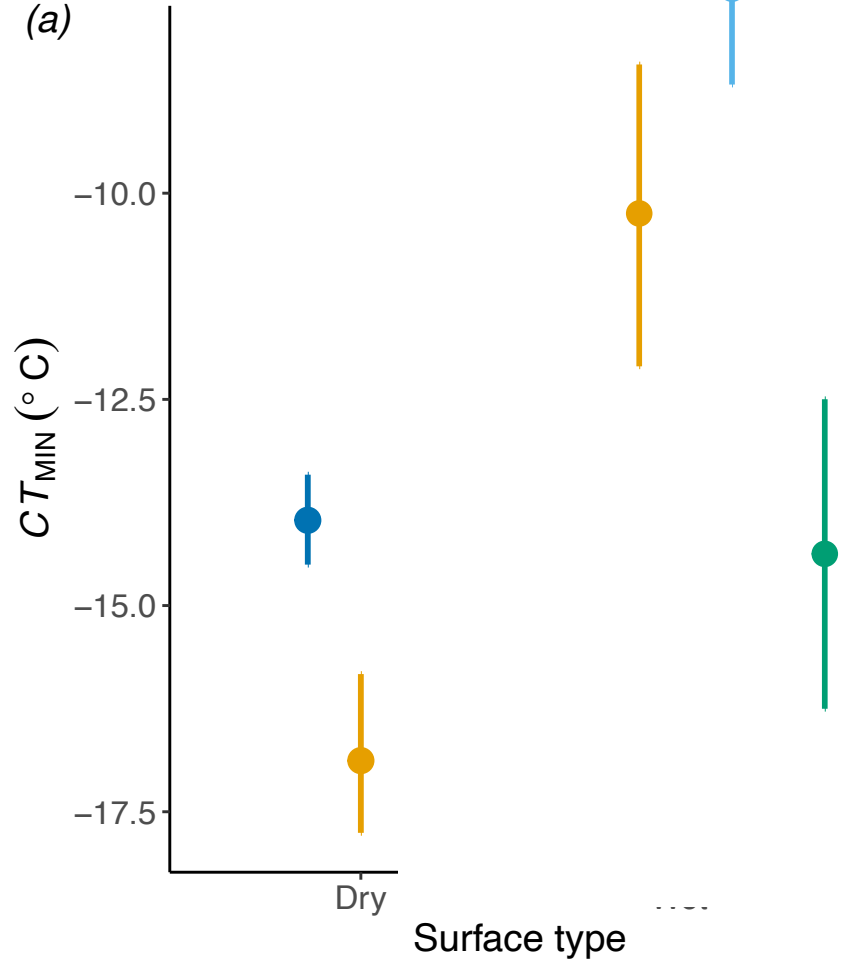
801

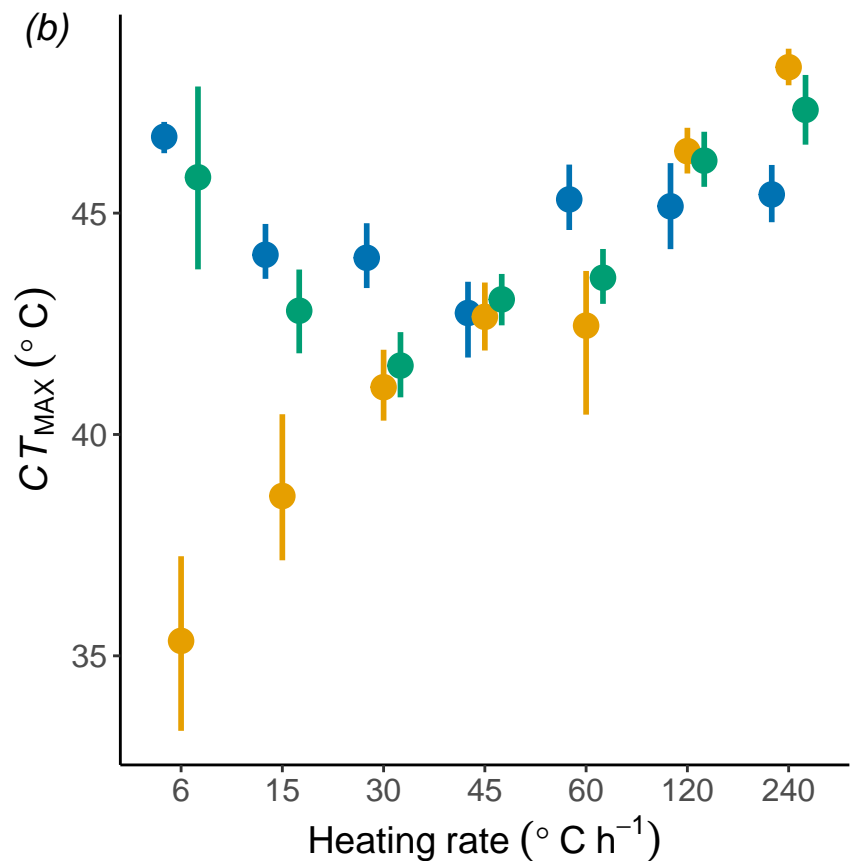
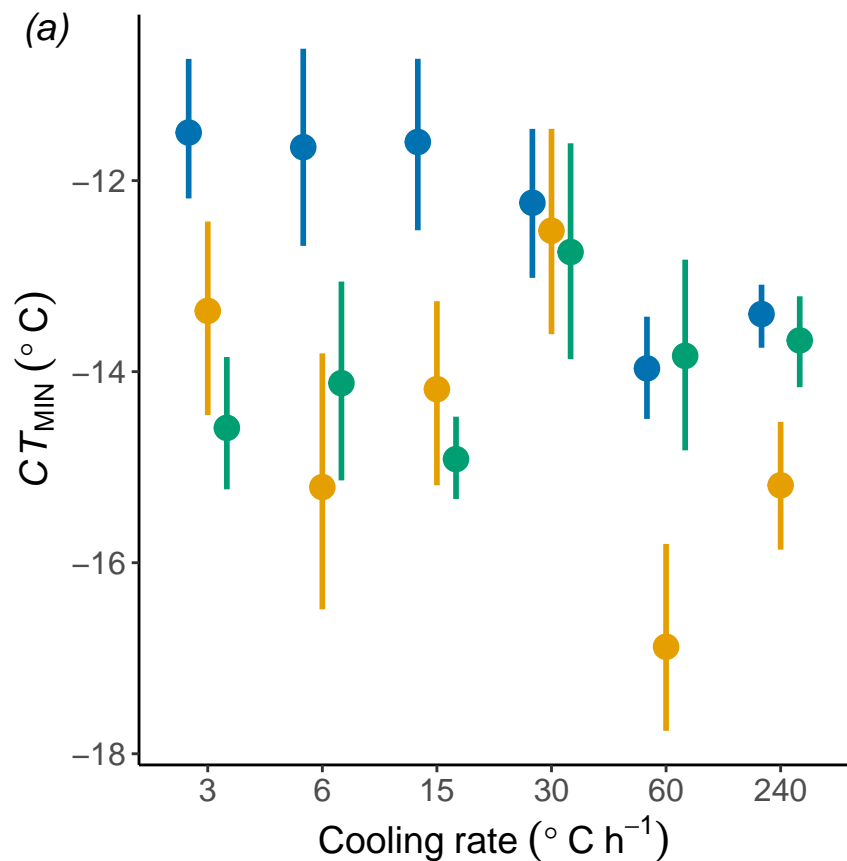
802 **Fig. 3.** The effect of varying heating/cooling rate (°C h<sup>-1</sup>) on the  $CT_{\text{MIN}}$  and  $CT_{\text{MAX}}$  estimates  
803 (°C) from basal chlorophyll fluorescence ( $F_0$ , relative units) of leaves. We tested how (a)  $CT_{\text{MIN}}$   
804 and (b)  $CT_{\text{MAX}}$  estimates of leaves from three plant species were affected by changing the  
805 temperature stress at different heating/cooling rates. Data points are means and 95% CIs that  
806 overlay raw data ( $n = 6$ –20 per treatment  $\times$  species combination).

807

808 **Fig. 4.** The effect of heating/cooling rate (°C h<sup>-1</sup>) as a continuous variable on the (a) predicted  
809  $CT_{\text{MIN}}$  and (b) predicted  $CT_{\text{MAX}}$  estimates (°C) in leaves from three plant species. Data points  
810 are means and 95% CIs ( $n = 6$ –20 per treatment  $\times$  species combination) with predicted response  
811 curves modelled with quadratic functions separately for each species.







Species ● *Escallonia rubra* ● *Melaleuca citrina* ● *Wahlenbergia ceracea*

